REPORT DOCUMENTATION PAGE

Form Approved OMB NO. 0704-0188

1. REPORT DATE (DD-MM-YYYY)	2. REPORT TYPE	3. DATES COVERED (From - To)
02-03-2017	Final Report	10-Jun-2013 - 9-Jul-2016

4. TITLE AND SUBTITLE
Final Report: Three Dimensional Nanopillar Optical Antenna Avalanche Detectors

5a. CONTRACT NUMBER
W911NF-13-1-0188

5b. GRANT NUMBER

5c. PROGRAM ELEMENT NUMBER
611102

6. AUTHORS
Alan C. Farrell, Pradeep N. Senanayake, Diana L. Huffaker

5d. PROJECT NUMBER

5e. TASK NUMBER

5f. WORK UNIT NUMBER

7. PERFORMING ORGANIZATION NAMES AND ADDRESSES
University of California - Los Angeles
Office of Contract and Grant Administration
11000 Kinross Avenue, Suite 211
Los Angeles, CA 90095 -1406

8. PERFORMING ORGANIZATION REPORT NUMBER

9. SPONSORING/MONITORING AGENCY NAME(S) AND ADDRESS (ES)
U.S. Army Research Office
P.O. Box 12211
Research Triangle Park, NC 27709-2211

10. SPONSOR/MONITOR'S ACRONYM(S)
ARO

11. SPONSOR/MONITOR'S REPORT NUMBER(S)
64436-EL-DRP.9

12. DISTRIBUTION AVAILIBILITY STATEMENT
Approved for Public Release; Distribution Unlimited

13. SUPPLEMENTARY NOTES
The views, opinions and/or findings contained in this report are those of the author(s) and should not contrued as an official Department of the Army position, policy or decision, unless so designated by other documentation.

14. ABSTRACT
Avalanche photodetectors (APDs) operating at 1064 nm are an integral component of light detection and ranging (LiDAR) systems used in imaging technologies such as acquisition tracking and pointing (ATP) and airborne topographic mapping. Current state-of-the-art APDs utilize a separate absorption-multiplication (SAM) structure using an In0.53Ga0.47As absorber lattice-matched to an InP multiplication layer. When operated in Geiger mode, these detectors are limited by the dark count rate caused by generation current in the InGaAs, making low-temperature operation necessary. At low temperature, trap-assisted tunneling (TAT) in the InP limits the

15. SUBJECT TERMS
Nanopillars, single photon avalanche detectors, geiger mode

16. SECURITY CLASSIFICATION OF:			17. LIMITATION OF ABSTRACT	15. NUMBER OF PAGES	19a. NAME OF RESPONSIBLE PERSON
a. REPORT	b. ABSTRACT	c. THIS PAGE			Diana Huffaker
UU	UU	UU	UU		19b. TELEPHONE NUMBER: 310-206-0853

Report Title

Final Report: Three Dimensional Nanopillar Optical Antenna Avalanche Detectors

ABSTRACT

Avalanche photodetectors (APDs) operating at 1064 nm are an integral component of light detection and ranging (LiDAR) systems used in imaging technologies such as acquisition tracking and pointing (ATP) and airborne topographic mapping. Current state-of-the-art APDs utilize a separate absorption-multiplication (SAM) structure using an In0.53Ga0.47As absorber lattice-matched to an InP multiplication layer. When operated in Geiger mode, these detectors are limited by the dark count rate caused by generation current in the InGaAs, making low-temperature operation necessary. At low temperature, trap-assisted tunneling (TAT) in the InP limits the performance. Although in theory it is possible to reduce generation current in the InGaAs by reducing the indium fraction (while still effectively absorbing at 1064 nm), in practice the reduction of bulk generation current is offset by the poor material quality resulting from lattice mis-matched growth on InP. In this work, we investigate the nanowire platform as a means to overcome this limitation. By taking advantage of the ability to grow high quality lattice mis-matched materials using selective-area epitaxy, two key design improvements are implemented: 1) the indium composition of the absorber is reduced to 30%, and 2) the InP multiplication region is replaced by GaAs. The reduced indium content in the InGaAs absorber reduces generation current by two orders of magnitude, while the GaAs produces a faster avalanche response compared to InP. This results in reduction in DCR by a factor of 1000 and a count rate > 1 MHz. Geiger mode characterization will be presented in detail, including dark count rate and photon detection rate.

Enter List of papers submitted or published that acknowledge ARO support from the start of the project to the date of this printing. List the papers, including journal references, in the following categories:

(a) Papers published in peer-reviewed journals (N/A for none)

Received		Paper
03/01/2017	5	Alan C. Farrell, Pradeep Senanayake, Xiao Meng, Nick Y. Hsieh, and Diana L. Huffaker. Diode characteristics approaching bulk limits in vertically-aligned GaAs nanowire array p-n junction photodiodes, Nano Letters (under review), ( ): . doi:
TOTAL:	**1**	

Number of Papers published in peer-reviewed journals:

(b) Papers published in non-peer-reviewed journals (N/A for none)

Received		Paper
TOTAL:	**1**	

Number of Papers published in non peer-reviewed journals:

(c) Presentations

Number of Presentations: 0.00

Non Peer-Reviewed Conference Proceeding publications (other than abstracts):

Received		Paper
03/01/2017	6	Alan C. Farrell, Baolai Liang, Xiao Meng, and Diana L. Huffaker. Nanowire separate absorption-multiplication avalanche photodetectors operating at 1064 nm, Photonics WEst. 28-JAN-17, San Francisco, CA. : ,
03/01/2017	7	Diana L. Huffaker, Alan C. Farrell, Pradeep Senanayake, Georges El-Howayek, Majeed Hayat. Dead-space effect in InGaAs nanopillar avalanche photodetectors, Nanowires 2015. 26-OCT-15, Barcelona, Spain. : ,
03/01/2017	8	Alan C. Farrell, Pradeep Senanayake, Georges El-Howayek, Majeed Hayat & Diana L. Huffaker. Dead-space effect in InGaAs nanopillar avalanche photodetectors, CSW 2015. 01-JUL-15, Santa Barbara, CA. : ,
TOTAL:	**3**	

Number of Non Peer-Reviewed Conference Proceeding publications (other than abstracts):

Peer-Reviewed Conference Proceeding publications (other than abstracts):

Received		Paper
03/01/2017	1.00	Alan C Farrell, Pradeep Senanayeke, Chung-Hong Hung, Marc Currie, Diana L. Huffaker. Reflection Spectromicroscopy for the Design of Nanopillar Optical Antenna Detectors, Device Research Conference. 23-JUN-14, Santa Barbara, CA. : ,
TOTAL:	**1**	

Number of Peer-Reviewed Conference Proceeding publications (other than abstracts):

(d) Manuscripts

Received	Paper
TOTAL:	

Number of Manuscripts:

Books

Received Book

TOTAL:

Received Book Chapter

TOTAL:

Patents Submitted

Plasmonically enhanced nanopillar separate absorpition multiplication diodes (PEN-SAMD)
UCLA Case No. 2012-531-2

Patents Awarded

Awards

Graduate Students

NAME	PERCENT_SUPPORTED	Discipline
Hyunseok Kim	0.49	
FTE Equivalent:	**0.49**	
Total Number:	**1**	

Names of Post Doctorates

NAME	PERCENT_SUPPORTED
Pradeep Senanayake	0.45
Wook-Jae Lee	1.00
FTE Equivalent:	**1.45**
Total Number:	**2**

Names of Faculty Supported

NAME	PERCENT_SUPPORTED	National Academy Member
Diana L. Huffaker	0.26	
FTE Equivalent:	**0.26**	
Total Number:	**1**	

Names of Under Graduate students supported

NAME	PERCENT_SUPPORTED	Discipline
Nick Hsieh	0.49	Electrical Engineering
FTE Equivalent:	**0.49**	
Total Number:	**1**	

Student Metrics

This section only applies to graduating undergraduates supported by this agreement in this reporting period

The number of undergraduates funded by this agreement who graduated during this period: 0.00

The number of undergraduates funded by this agreement who graduated during this period with a degree in science, mathematics, engineering, or technology fields:..... 1.00

The number of undergraduates funded by your agreement who graduated during this period and will continue to pursue a graduate or Ph.D. degree in science, mathematics, engineering, or technology fields:..... 0.00

Number of graduating undergraduates who achieved a 3.5 GPA to 4.0 (4.0 max scale):..... 1.00

Number of graduating undergraduates funded by a DoD funded Center of Excellence grant for Education, Research and Engineering:..... 0.00

The number of undergraduates funded by your agreement who graduated during this period and intend to work for the Department of Defense 0.00

The number of undergraduates funded by your agreement who graduated during this period and will receive scholarships or fellowships for further studies in science, mathematics, engineering or technology fields:..... 0.00

Names of Personnel receiving masters degrees

NAME
Total Number:

Names of personnel receiving PHDs

NAME
Total Number:

Names of other research staff

NAME	PERCENT_SUPPORTED
FTE Equivalent:	
Total Number:	

Sub Contractors (DD882)

Inventions (DD882)

Scientific Progress

See Attachment

Technology Transfer

Abstract

The nanopillar optical antenna avalanche detectors (NOAADs) produced by this effort will address the need for high performance detectors for SWIR focal plane arrays for both passive and active imaging. Our proposed approach combines plasmonically enhanced absorption due to a nanopillar optical antenna with a nanoscale multiplication region. We previously demonstrated both high external quantum efficiency and low excess noise in linear mode operation of InGaAs avalanche photodetectors (APDs). We now turn to Geiger mode operation of single photon avalanche detectors (SPADs). UCLA has developed the growth of separate absorption-multiplication (SAM) APDs, consisting of lattice mis-matched InGaAs absorbers on GaAs avalanche regions. Temperature dependent dark current measurements on fabricated detectors show that the electric field is confined within the avalanche region before punch-through, with a strong photoresponse at 1064 nm above punch-through. We measure a dark count rate (DCR) less than 10 Hz at 77 K in *free running mode*, comparable to commercial silicon SPADs and over 10^3 lower than commercial InGaAs/InP SPADs. A pulse-width under 200 ns indicates count rates greater than 1 MHz are possible, over 10 times faster than commercial InGaAs/InP SPADs. Finally, we show a time sweep of the device under dark and illuminated conditions, and a clear increase in the number of counts is observed when 1064 nm incident light is applied.

Scientific Progress and Accomplishments

Heteroepitaxy of InGaAs absorber on GaAs avalanche region

All-axial $In_{0.27}Ga_{0.73}As$ was grown on GaAs avalanche layers using triethygallium (TEGa) rather than the commonly used trimethylgallium (TMGa). The use of TEGa as a precursor significantly reduced radial overgrowth of InGaAs, which has been a significant obstacle to achieving high performance SAM-APDs. Figure 1a shows a schematic of the intended structure. The avalanche region is grown first at 680° C using unintentionally p-type GaAs. A p-GaAs field control layer is then grown by using diethyzinc (DEZn) as a p-dopant. The InGaAs absorber is grown at the same temperature as the GaAs, with a 30% gas phase indium composition at a V/III ratio of 40, then a contact layer is grown using p-InGaAs. Finally, an InGaP passivation shell is grown at 600° C. Figure 2b shows a tilted SEM images of as-grown nanowires with a 400 nm InGaAs layer. The diameter of the nanowires before and after growth of InGaAs was measured and found to be the same, indicating no radial growth occurred. Figure 2c shows the result of growing a 600 nm InGaAs layer. In this case, a small percentage of the nanowires are curved, caused by radial growth of InGaAs over the GaAs. The strain resulting from the lattice mis-matched interface causes the nanowires to bend. Figure 1d shows an STEM image along with an EDS scan along the length of the nanowire. The InGaAs region is clearly visible as the bright region at the top of the nanowire. EDS confirms that the indium composition is 27% and that the composition is uniform.

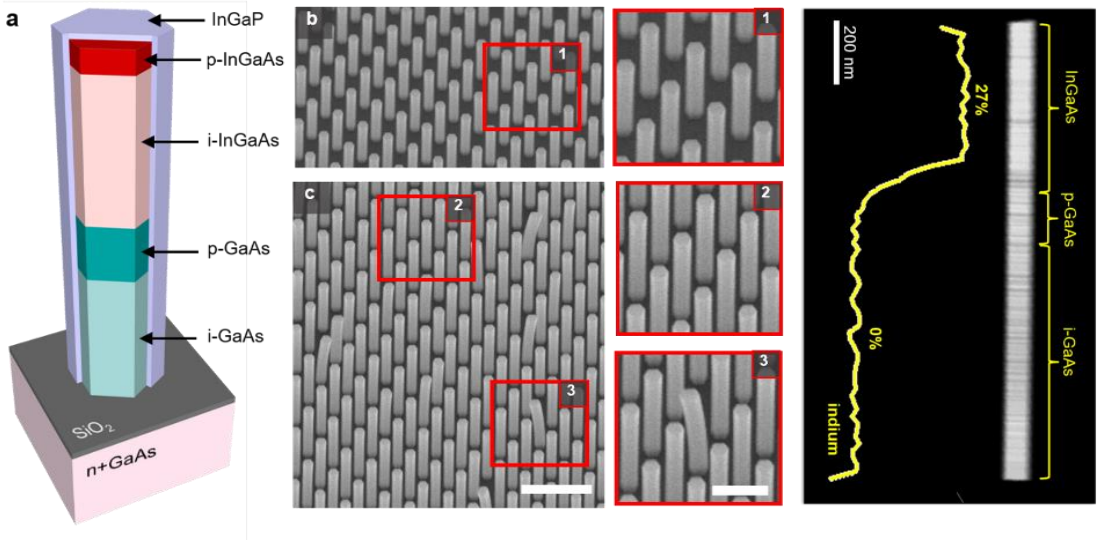

Figure 1 | a, Schematic of nanowire SAM-APD structure. **b,** Tilted scanning electron micrograph (SEM) of array of InGaAs/GaAs nanowire SAM-APDs with 400 nm InGaAs layer. **c,** Tilted scanning electron micrograph (SEM) of array of InGaAs/GaAs nanowire SAM-APDs with 600 nm InGaAs layer. Scale bar: 800 nm, Inset scale bar: 400 nm. **d,** STEM and EDS of single nanowire showing all-axial heteroepitaxy of InGaAs on GaAs.

Dark current and avalanche breakdown

Temperature-dependent dark current measurements, shown in Figure 2a, were performed in order to determine the source of the leakage current before punch-through. The dark current rapidly drops from 800 pA at 300 K to 100 fA at 175 K at 10 V reverse bias. Figure 2b shows an Arrhenius plot of the leakage current at 100 mV reverse bias and compares an InGaAs photodetector, a GaAs photodetector, and the InGaAs/GaAs SAM-APD. Note that the activation energy of the SAM-APD is the same as that of the GaAs photodetector, indicating that the electric field is confined entirely within the GaAs avalanche layer, despite the existence of an InGaAs layer above it.

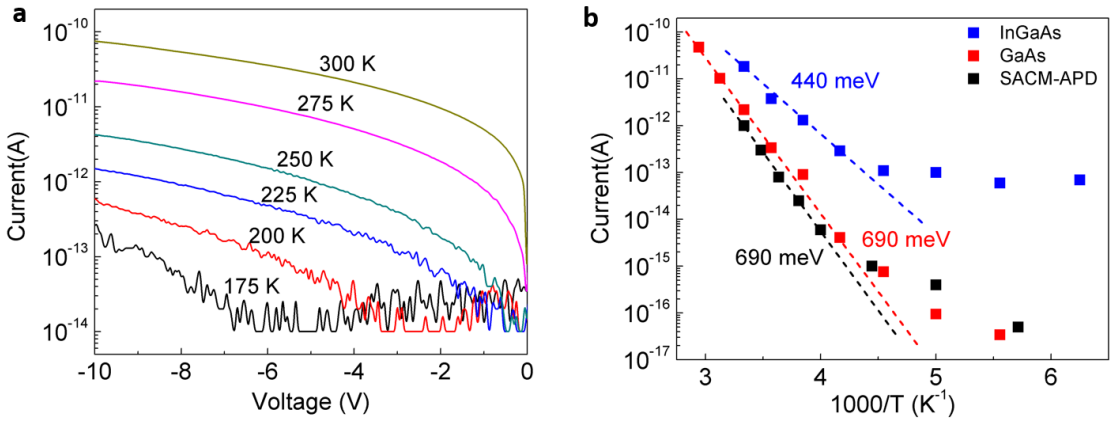

Figure 2 | a, Temperature-dependent dark current of an InGaAs/GaAs nanowire SAM-APD. **b,** Arrhenius plot of the leakage current at 100 mV reverse bias showing that the activation energy of the SAM-APD is the same as that of the GaAs photodetector.

The nanowire SAM-APDS where then biased until breakdown, shown in Figure 3. The dark current is below the sensitivity of the measurement setup right up until the device breaks down. The breakdown voltage randomly shifts from a minimum of 17 V to a maximum of 22 V. This random shift in the breakdown voltage is a known phenomenon that occurs when the number of carriers available to initiate avalanche breakdown is very small, on the order of 10 per second. With the number of carriers being so low, as the DC sweep reaches the breakdown voltage, there isn't always a carrier available to initiate avalanche breakdown before the next step in the DC sweep is reached. Thus, the device can frequently be biased several volts above the breakdown voltage before avalanche actually occurs. Note that avalanche breakdown in nanowire devices typically leads to device degradation, however in this case, the nanowire SAM-APD went through twenty DC sweeps taken to breakdown with now signs of degradation. The relatively low current at breakdown of 1 nA or less, is likely a result of only a single nanowire breaking down during every sweep. We can take advantage of this characteristic to reduce after-pulsing in SPADs, which is caused by trap filling and releasing after an avalanche pulse.

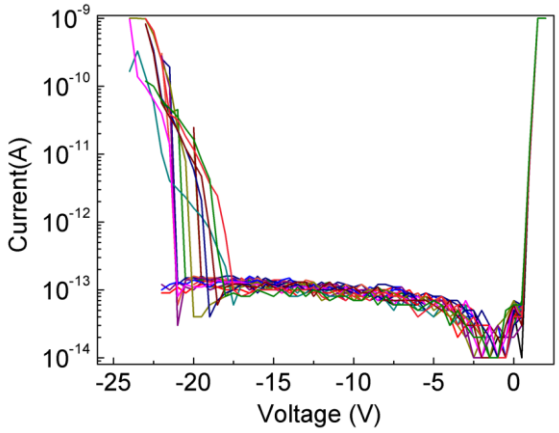

Figure 3 | a, Repeated measurements of the dark I-V on a single nanowire SAM-APD. The breakdown voltage randomly shifts between 17 V and 22 V reverse bias. The random shift is due to the extremely low dark current, or equivalently, the low probability of the random carrier generation required to initiate avalanche breakdown.

Single photon avalanche detector operating in free-running mode

With the appropriate supporting circuitry, the nanowire SAM-APD can by transformed into a SPAD. The device was passively quenched using a resistor in series with the SPAD, and the dark and photon counts were measured in *free-running mode*, i.e., no gate or dead time was used. Figure 4 shows the pulse-shape of dark counts for increasing reverse bias. The full-width half-max is less than 200 ns, indicating that count rates greater than 1 MHz are possible. The appearance of a secondary peak during the fall time is due to secondary avalanche events that occur before the potential across the SPAD has dropped below the breakdown voltage.

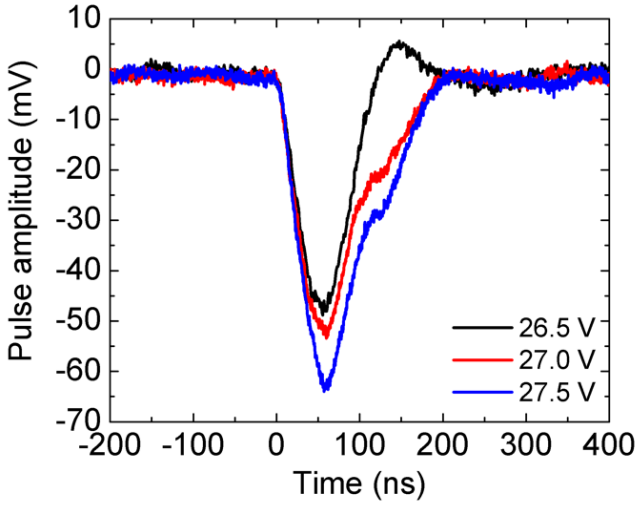

Figure 4 | Temporal pulse shape of dark counts for increasing bias. The FWHM is less than 200 ns, indicating that count rates greater than 1 MHz are possible.

The DCR was measured at 77 K as a function of increasing bias. As the electric field increases within the nanowire, so too does the breakdown probability, resulting in an increase in the DCR. Figure 5 shows the DCR vs. bias for a representative device. Even at a reverse bias of 29 V, which is 7 V above breakdown, the DCR is only 6 Hz! Not only is this extremely low, but this was achieved without the use of the standard active quenching circuits required to suppress after-pulsing in commercial InGaAs/InP SPADs. A DCR this low without afterpulsing effects allows much higher density pixel arrays, since complicated and space occupying quenching circuitry is not required.

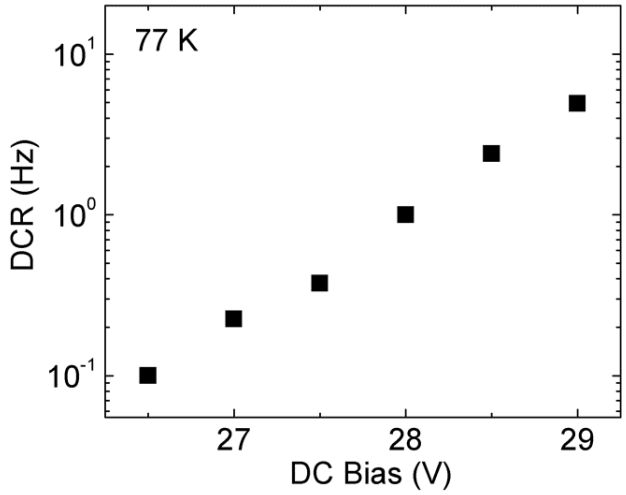

Figure 5 | a, Repeated measurements of the dark I-V on a single nanowire SAM-APD. The breakdown voltage randomly shifts between 17 V and 22 V reverse bias. The random shift is due to the extremely low dark current, or equivalently, the low probability of the random carrier generation required to initiate avalanche breakdown.

Figure 6 shows a 10 second time sweep of the voltage across the load resistor under dark and illuminated conditions using a real-time high-speed oscilloscope. Each pulse in the top figure is triggered by a dark carrier, and represents a time domain view of the DCR, i.e., adding all the pulses and dividing by the total time gives the DCR, which in this case is about 3 Hz. In the figure below, the device is illuminated with a 1064 nm diode laser. There is a clear increase in the number of pulses compared to the dark conditions, rising to about 20 Hz. This ability to detect photons in free-running mode has far reaching consequences. For example, current commercial InGaAs/InP SPADs must employ active quenching in order to suppress afterpulsing. This additional circuitry must accompany *each* individual pixel in a focal plane array. This results in a very large pixel pitch, which in turn, makes InGaAs/InP SPAD arrays very large, low resolution, and expensive. Another advantage of free-running mode operation is that the count rate is no longer limited by the dead time (the amount of time the SPAD is biased below breakdown to allow all traps to be released), but by the *pulse width*. This can increase the count rate from less than 100 kHz in commercial SPADs to over 5 MHz in nanowire SPADs.

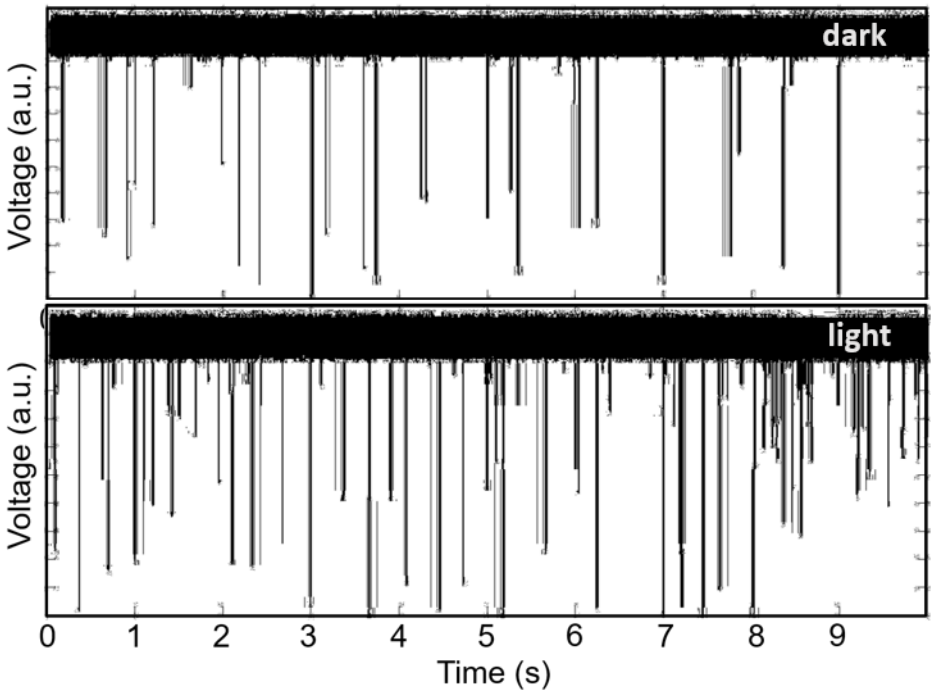

Figure 6 | Time sweep spanning 10 seconds using a high-speed real-time oscilloscope. The top and bottom figures are under dark and illuminated conditions, respectively. The light source was a 1064 nm diode laser.